Structural Evaluation of Tandem Hairpin Pyrrole−Imidazole Polyamides Recognizing Human Telomeres

Akiyoshi Hirata,[†] Kiyoshi Nokihara,[*,†] Yusuke Kawamoto,[‡] Toshikazu Bando,[‡] Asuka Sasaki,[§] Satoru Ide,[§] Kazuhiro Maeshima,[§] Takeshi Kasama,[∥] and Hiroshi Sugiyama[‡,⊥]

[†]HiPep Laboratories, Nakatsusaka-cho 486-46, Kamigyo-ku Kyoto, 602-8158, Japan

[‡]Department of Chemistry, Graduate School of Science, Kyoto University, Sakyo, Kyoto 606-8502, Japan

[§]Biological Macromolecules Laboratory, Structural Biology Center, National Institute of Genetics, and Department of Genetics, School of Life Science, Graduate University for Advanced Studies (Sokendai), Mishima, Shizuoka 411-8540, Japan

[∥]Research Center for Medical and Dental Sciences, Tokyo Medical and Dental University, Tokyo, Japan

[⊥]Institute for Integrated Cell-Material Science (WPI-iCeMS), Kyoto University, Sakyo, Kyoto 606-8501, Japan

S *Supporting Information*

ABSTRACT: A polyamide containing *N*-methylpyrrole (Py) and *N*-methylimidazole (Im), designated PIPA, binds with high affinity and specificity to specific nucleotide sequences in the minor groove of double-helical DNA. Based on a recent report of the synthesis of PIPA for telomere visualization, the present paper focused on the size of the connecting part (hinge region) of two PIPA segments of the tandem hairpin PIPA, Dab(Im-Im-Py)-Py-Py-Py-Im-[Hinge]-Dab(Im-Im-Py)-Py-Py-Py-Im-βAla-NH(CH$_2$)$_3$N(CH$_3$)-(CH$_2$)$_3$NH-[Dye]. The present paper also describes the characterization of binding by measuring the thermal melting temperature and surface plasmon resonance and by specific staining of telomeres (TTAGGG)n in human cells. Micro-

heterogeneity was also investigated by high-resolution mass spectrometry. We found that the optimal compound as the hinge segment for telomere staining was [-NH(C$_2$H$_4$O)$_2$(C$_2$H$_4$)CO-] with tetramethylrhodamine as the fluorescent dye.
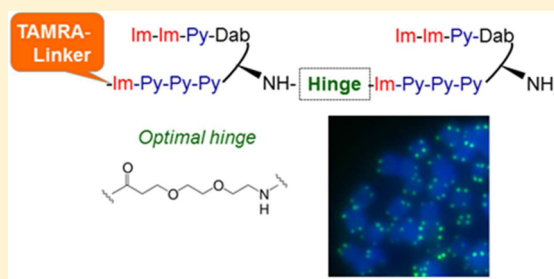
INTRODUCTION

A polyamide containing *N*-methylpyrrole (Py) and *N*-methylimidazole (Im), designated PIPA, binds with high affinity and specificity to specific nucleotide sequences in the minor groove of double-helical DNA.[1] For efficient binding to long sequences, β-alanine residues are introduced to match the pitch of the DNA base pairs and to act as an aliphatic substitution for a Py ring.[2] In addition to the C-terminal β-alanine, γ-aminobutyric acid, and 2,4-diaminobutyric acid (Dab) residues recognize an A·T or T·A base pair.[3] During the past two decades, much attention has been devoted to the synthesis[4] and characterization,[5] of PIPA. The hairpin is one versatile PIPA structure that has been developed[6] to increase the number of base pairs recognized by PIPA and its specificity.[7] Some hairpins have been developed to connect the two polyamide subunits via a hinge and the amino group of Dab of the α position, designated as a tandem hairpin polyamide.[8]

In eukaryotic cells, the telomeres protect the ends of chromosomes. The number of telomere repeats decreases with cell division, relating to the aging process or tumorigenesis. The telomere length is one important biomarker to examine these processes. Therefore, development of fluorescently labeled PIPAs, which target telomeres, has attracted strong interest for visualization and measurement of telomere length.[9] A tandem hairpin PIPA probe to identify telomeres was reported initially by Maeshima, Janssen, and Laemmli.[10] Significant progress has not been achieved, and no useful probes are commercially available. Some antibody-based telomere staining is indeed available. However, telomere staining by PIPAs is different from the antibody−telomere staining because of the following reasons: The PIPAs directly target the telomeric repeats, but the antibody can recognize the proteins that bind to the telomeric repeats (e.g., TRF1 proteins). This means that the signal intensity of the antibody staining does not necessary mean the telomere length. To measure the telomere length, cell biologists have so far used telomere FISH (fluorescence in situ hybridization) with a peptide nucleic acid (PNA) oligonucleotide probe,[11] which normally denatures DNA under harsh conditions. Notably, the harsh conditions of FISH present a risk that can lead to destruction of the telomere structure. One of the biggest advantages of PIPAs is rapid and simple telomere staining under mild conditions. Very recently, Sugiyama and co-workers succeeded in preparing conjugates of PIPA and functional molecules.[12] In particular, fluorescently labeled PIPAs targeting human and mouse telomeres have been developed using the building block method and have shown
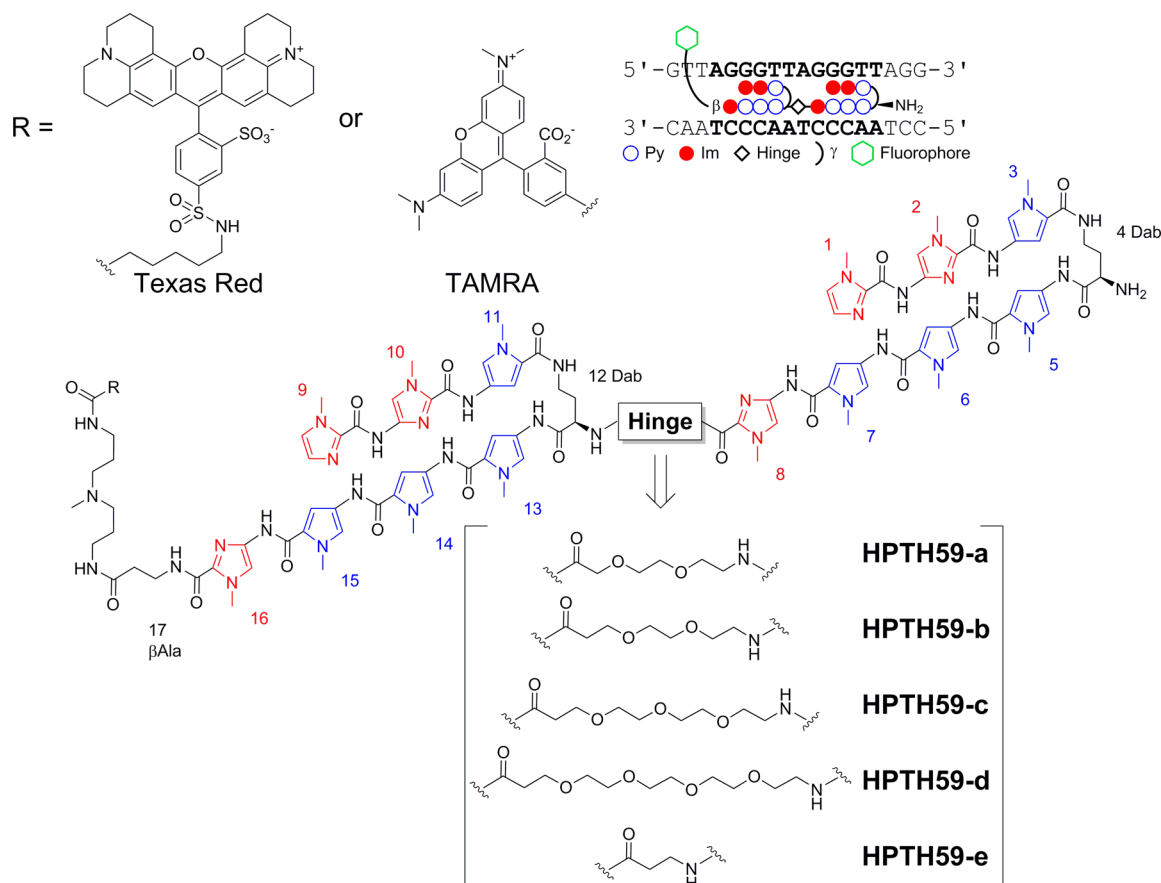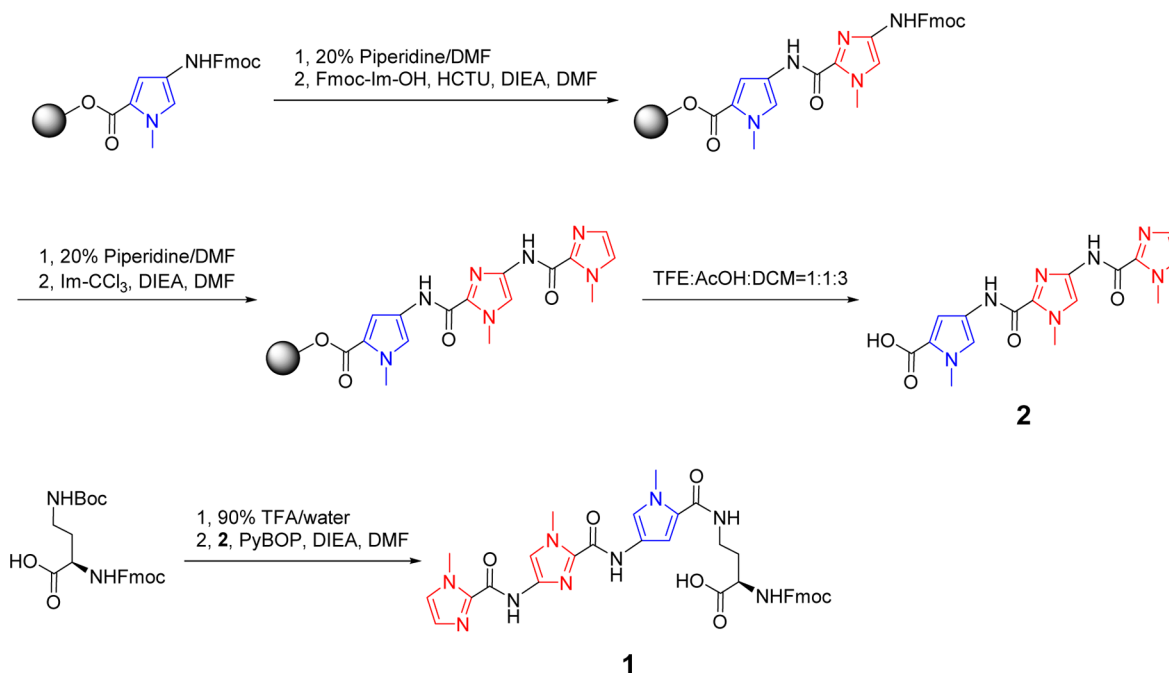
Figure 1. Synthetic PIPA library used in the present study and its ball-and stick representation. The numbers indicate the residues of building blocks from the amino terminus that were incorporated as nonproteinogenic amino acids. TAMRA is tetramethylrhodamine.

Scheme 1. Synthetic Route to Building Block 1

that the telomere length at the single telomere level is related to the abundance of TRF1 protein, a shelterin complex component.[12a] The synthetic target PIPA has a hinge segment whose size has not yet been optimized. Hence, the size of the

hinge seemed to be important for matching the TTAGGG-seq repeat, and recently several PEG-based linkages have often been used in chemical biology; thus, we have attempted to use different sizes. PIPA has advantages over siRNA or PNAs

11547

dx.doi.org/10.1021/ja506058e | J. Am. Chem. Soc. 2014, 136, 11546−11554

complexes; that is, PIPA is nuclease resistant[13] and enters cell nuclei without needing any delivery system.[14]

The present paper describes the syntheses of several tandem hairpin PIPAs, Dab(Im-Im-Py)-Py-Py-Py-Im-[Hinge]-Dab(Im-Im-Py)-Py-Py-Py-Im-βAla-NH(CH$_2$)$_3$N(CH$_3$)-(CH$_2$)$_3$NH-[Dye], comprising different-sized hinge segments, designated Dye **HPTH59-a−e** (illustrated in Figure 1). We have characterized these PIPAs by measuring their thermal melting temperatures and have compared their binding affinities by surface plasmon resonance (SPR) experiments in addition to the staining of telomeres. PIPA seemed to not be highly stable during syntheses, but byproducts have not been previously reported. Biomolecules, except for small sizes, may have microheterogeneity,[15] which has also been investigated by high-resolution mass spectrometry (MS).

■ RESULTS AND DISCUSSION

Design and Construction of Libraries. The syntheses were performed based on a recently reported[12a] method except that the short fragment Im-Im-Py-OH (**2**) was prepared by the solid-phase synthesis (SPS) to achieve effective production to give Fmoc-D-Dab(Im-Im-Py)-OH (**1**) (described in Scheme 1). The resulting fragments Fmoc-Py-OH, Fmoc-Im-OH, and Fmoc-Py-Im-OH were prepared in solution and were used as the building blocks for SPS. Five different sizes of hinge segment were used with two different fluorescent dyes to provide diversity to optimize this particular telomere-visualizing probe. Building block **2** was prepared by SPS using 2-chlorotrityl resin and was cleaved to give the desired trimer in a good yield. This material was introduced to the side-chain amino group of Fmoc-D-Dab-OH to give **1**, which was purified on a silica gel column and used as a building block. Polyamide assembly was performed successfully on an automated synthesizer (PSSM-8, Shimadzu) from the starting resin Fmoc-βAla-Wang. Five different hinge segments were also incorporated as Fmoc-oxyethylene carboxylic acid derivatives (**HPTH59-a**, **-b**, **-c**, and **-d**), and Fmoc-βAla-OH was used for **HPTH59-e**. Cleavage with 3,3′-diamino-N-methyldipropylamine was followed by purification using reversed-phase (RP)-HPLC and gave Dab(Im-Im-Py)-Py-Py-Py-Im-[Hinge]-Dab(Im-Im-Py)-Py-Py-Py-Im-βAla-NH(CH$_2$)$_3$N(CH$_3$)-(CH$_2$)$_3$-amine. The fluorophore group was incorporated as a succinimidyl ester. The α-amino group of Dab is not highly reactive because of steric hindrance, and thus side-chain protection was not required.
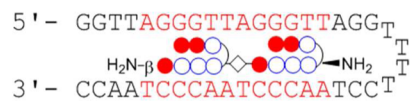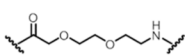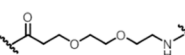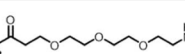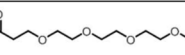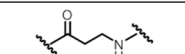
Binding Affinities and Specificities of Polyamides with Different-Sized Hinge Segments. The thermal stabilization of the polyamide−DNA complex can be analyzed by thermal melting temperature (T_m) analysis, which measures the relative binding affinity, and can discriminate between mismatched sequences.[16] Thermal denaturation analysis of DNA and of the polyamide−DNA complexes was performed to evaluate the strength and specificity of the binding of the present library (**HPTH59-a−e**) to telomeric repeats. The results are summarized in Table 1. The ΔT_m values of **HPTH59-a**-ODN-1/2, **-b**-ODN-1/2, **-c**-ODN-1/2, **-d**-ODN-1/2, and **-e**-ODN-1/2 were 26.8, 27.1, 23.6, 23.0, and 20.3 °C, respectively, demonstrating that these polyamides can bind to TTAGGG repeats. The affinity was in the order **HPTH59-a** and **-b** > **-c** > **-d** > **-e**, presumably because of the hinge length.[8c] The ΔT_m (match) − ΔT_m (mismatch) ($\Delta\Delta T_m$) values of **HPTH59-a**-ODN-3/4, **-b**-ODN-3/4, **-c**-ODN-3/4, **-d**-ODN-3/4, and **-e**-ODN-3/4 were 11.0, 11.3, 9.7, 10.2, and 9.0 °C,

Table 1. Results of T_m Analyses^a

dsDNA	HPTH59-a [°C] T_m	ΔT_m	$\Delta\Delta T_m$	HPTH59-b [°C] T_m	ΔT_m	$\Delta\Delta T_m$	HPTH59-c [°C] T_m	ΔT_m	$\Delta\Delta T_m$	HPTH59-d [°C] T_m	ΔT_m	$\Delta\Delta T_m$	HPTH59-e [°C] T_m	ΔT_m	$\Delta\Delta T_m$
ODN-1/2 T_m: 44.8 °C (±0.2 °C)	71.6 (±0.0)	26.8	—	71.9 (±0.4)	27.1	—	68.4 (±0.3)	23.6	—	67.8 (±0.2)	23.0	—	65.1 (±0.3)	20.3	—
ODN-3/4 T_m: 47.3 °C (±0.1 °C)	63.1 (±0.2)	15.8	11.0	63.1 (±0.1)	15.8	11.3	61.2 (±0.2)	13.9	9.7	60.1 (±0.2)	12.8	10.2	58.6 (±0.1)	11.3	9.0
ODN-5/6 T_m: 45.1 °C (±0.1 °C)	64.7 (±0.2)	19.6	7.2	63.1 (±0.1)	18.0	9.1	60.6 (±0.1)	15.5	8.1	59.5 (±0.3)	14.4	8.6	58.0 (±0.3)	12.9	7.4
ODN-7/8 T_m: 42.8 °C (±0.1 °C)	57.3 (±0.3)	14.5	12.3	54.8 (±0.3)	12.0	15.1	54.2 (±0.2)	11.4	12.2	52.2 (±0.3)	9.4	13.6	51.1 (±0.2)	8.3	12.0

^{a} $\Delta\Delta T_m$ = ΔT_m (match) − ΔT_m (mismatch), dsDNA: double strand DNA.

Table 2. Results of SPR Measurement

Hinge segment		k_a (M^{-1}s^{-1})	k_d (s^{-1})	K_D (M)	χ^2
HPTH59-a		1.7×10^6	1.6×10^{-3}	9.3×10^{-10}	0.28
HPTH59-b		2.9×10^5	2.5×10^{-3}	8.6×10^{-9}	0.29
HPTH59-c		2.3×10^5	4.3×10^{-3}	1.9×10^{-8}	0.55
HPTH59-d		1.1×10^5	3.9×10^{-3}	3.5×10^{-8}	0.33
HPTH59-e		7.6×10^4	4.9×10^{-3}	6.4×10^{-8}	0.75

respectively. By contrast, the $\Delta\Delta T_\mathrm{m}$ values of **HPTH59-a**-ODN-5/6, **-b**-ODN-5/6, **-c**-ODN-5/6, **-d**-ODN-5/6, and **-e**-ODN-5/6 were 7.2, 9.1, 8.1, 8.6, and 7.4 °C, respectively. The complexes of **HPTH59-a**, **-b**, **-c**, **-d**, and **-e** with ODN-7/8, which has a 2 bp mismatch, had higher $\Delta\Delta T_\mathrm{m}$ values: 12.3, 15.1, 12.2, 13.6, and 12.0 °C, respectively. These results suggest that polyamides can discriminate between a 1 bp and 2 bp mismatch, and that polyamides at the C-terminal side can discriminate better than those at the N-terminal side. Compared with the $\Delta\Delta T_\mathrm{m}$ values of **HPTH59-a**-ODN-5/6 and **HPTH59-b**-ODN-5/6, **HPTH59-b** had better selectivity for the target DNA sequences than **HPTH59-a**. These results indicate that the specificity of the polyamide at the N-terminal side was improved by modifying the hinge length. All present compounds recognized a 1 or 2 bp mismatch. The affinity of **HPTH59-b** was decreased by one methylene added to **HPTH59-a**, although this increased the discrimination of the mismatch. Thus, **HPTH59-b** would give a higher signal-to-noise (background) intensity ratio (S/N ratio) by reducing the background. Hence, both the affinity and mismatch recognition were reduced in **HPTH59-c**, and further elongation of the hinge segment in **HPTH59-d** decreased the affinity despite similar mismatch recognition. **HPTH59-e** with the shortest hinge segment had minimal affinity and mismatch recognition. Within the present hinge library, **HPTH59-b** was the best compound for mismatch discrimination, although the difference between **HPTH59-a** and **-b** was small.

Sequence-specific binding of the present library (**HPTH59-a–e**) was also evaluated by SPR experiments.[7e,17] The K_D values for **HPTH59-a–e** are summarized in Table 2. The K_D values were in the order **HPTH59-a** (9.3×10^{-10} M) < **HPTH59-b** (8.6×10^{-9} M) < **HPTH59-c** (1.9×10^{-8} M) < **HPTH59-d** (3.5×10^{-8} M) < **HPTH59-e** (6.4×10^{-8} M). These results demonstrated that **HPTH59-a** had the highest affinity for matching DNA. The size of the hinge segment was important for binding to telomeres. Other than **HPTH59-a** and **-b**, the affinity was consistent with the T_m analyses, in which **HPTH59-b** showed the highest affinity, although **HPTH59-a**

showed higher affinity in the SPR measurements, whereas DNAs were immobilized and influenced in this experiment.

Human Telomere Staining with Fluorescent PIPA. We doubly stained human HeLa 1.3 cell spreads with PIPAs and 4′,6-diamidino-2-phenylindole (DAPI) to compare the ability of the synthesized PIPAs (TAMRA-labeled **HPTH59-a**, TAMRA-labeled **HPTH59-b**, TAMRA-labeled **HPTH59-c**, and Texas Red-labeled **HPTH59-a**) to stain telomeres specifically. Cell spreads are often used for clinical karyotype tests and were prepared by methanol/acetic acid fixation. The images are shown in Figure 2. DAPI staining visualized the chromosomal bodies and nuclei, and PIPA staining showed many intense foci. In the chromosomes, two foci were observed at every chromosomal end (Figure 2B), suggesting that all four PIPAs could bind to the human telomeric repeat TTAGGG. The background signals from the nontelomeric regions decreased when stained, especially with TAMRA-labeled **HPTH59-b**. Similar results were obtained using HeLa 1.3 cells fixed by formaldehyde, a common fixative in cell biology (Figure 3). We observed many sharp foci in the nuclei (Figure 3A). The background could be compared easily between images. The surface plots (second row) based on the images in Figure 3B (second row) and their S/N ratios are shown in Figure 4 and suggest that TAMRA-labeled **HPTH59-b** staining had the highest S/N ratio. The cell staining data demonstrated that the human telomere targeting by PIPA was consistent with the results obtained from both the T_m and SPR analyses.

Investigation of Microheterogeneity. The quality assurance microheterogeneity of PIPA was investigated because the synthetic target material seemed to be relatively sensitive to oxygen. The HPLC profile of the purified Texas Red-labeled **HPTH59-a**, which had been freeze-dried and stored in the dark at −30 °C, indicated a single component (>95%), and the mass of the desired **HPTH59-a** was 2947.2438 Da (+0.95 ppm difference from the calculated mass). Hence, several minor peaks of oxidized compounds were envisaged (Figure 5).

The difficulty in the structural analysis of PIPA is described as follows. Most building blocks for the synthetic target PIPA
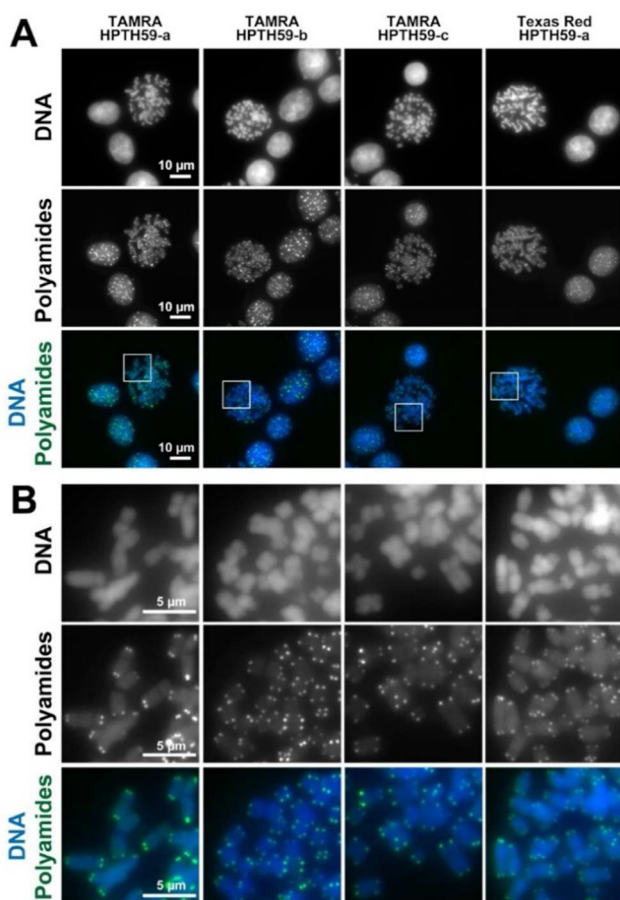
Figure 2. Telomere staining of HeLa 1.3 cells and cell spreads with fluorescent polyamides. HeLa 1.3 cell spreads were stained with DAPI (first row) and the fluorescent polyamides (second row): first column, TAMRA-labeled **HPTH59-a**; second column, TAMRA-labeled **HPTH59-b**; third column, TAMRA-labeled **HPTH59-c**; fourth column, Texas Red-labeled **HPTH59-a**. The merged images of DAPI and polyamide staining are shown in the third row. Enlarged images of the boxed regions in panel A are shown in panel B. All images are shown on the same intensity scale.

Figure 3. Telomere staining of HeLa 1.3 cells with fluorescent polyamides. HeLa 1.3 cells were stained with DAPI (first row) and the fluorescent polyamides (second row): first column, TAMRA-labeled **HPTH59-a**; second column, TAMRA-labeled **HPTH59-b**; third column, TAMRA-labeled **HPTH59-c**; fourth column, Texas Red-labeled **HPTH59-a**. The merged images of DAPI and polyamide staining are shown in the third row. Enlarged images of the boxed regions in panel A are shown in panel B. All images are shown on the same intensity scale.

are Im and Py, which differ by only 1 Da. Thus, byproducts have similar properties and, in many cases, the HPLC peaks overlap. The stability and characterization of the byproducts of synthetic PIPA have not been reported previously. Even tiny amounts of numerous oxidized compounds have been identified. Mass differences of 15.995 Da indicate one oxygen adduct on Texas Red-labeled **HPTH59-a**, which was envisaged at Py but not at Im residues of Texas Red-labeled **HPTH59-a** (Figure 6). One oxygen adduct was identified at residue no. 7 (Figure 7). Although the amounts are very small, these phenomena (oxygen adducts) were envisaged at Py residues but not at Im residues. Figure 8 indicates the pattern of oxygen adducts on purified Texas Red-labeled **HPTH59-a** as a single peak on HPLC. Even very small amounts of several oxidized compounds coeluted with the mother compound. The oxidized positions were different, although the signals were clearly visible by integration. Oxygen adducts occurred at various residues, which were deduced from multiple peaks as shown in Supporting Information (S9). Oxidation must be considered during treatments such as the assembly, purification, freeze-drying, and storage of PIPA.
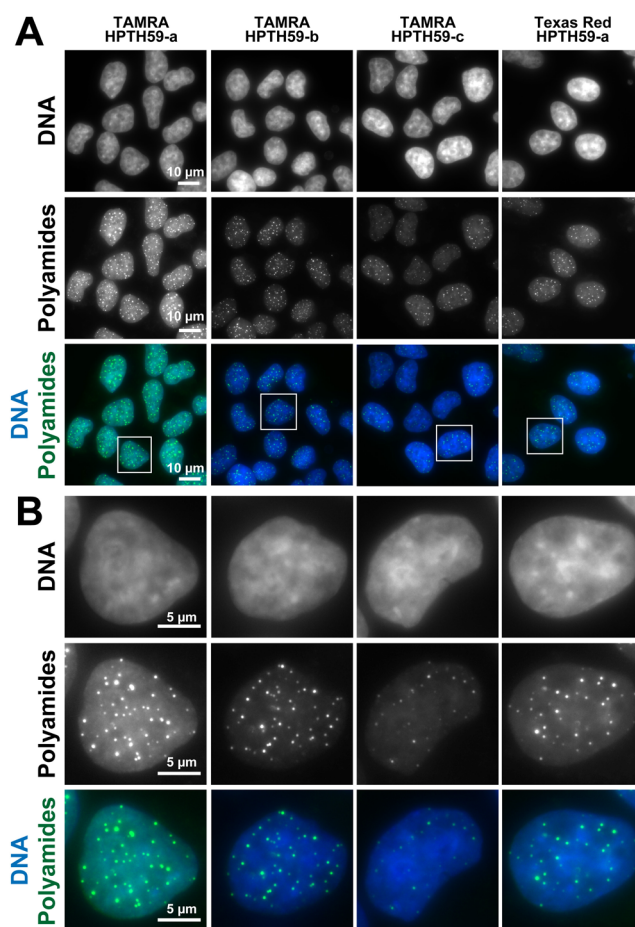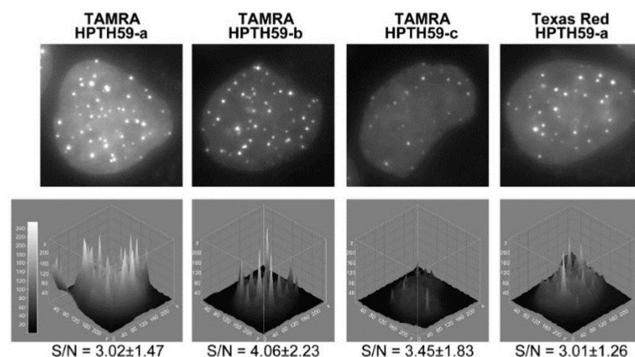

Figure 4. Signal-to-noise (S/N) ratios of the images. The surface plots (second row) are based on the images shown in Figure 3B (first row). These surface plots were drawn using ImageJ software (as interactive 3D surface plots). The S/N intensity ratios and SDs are shown at the bottom.
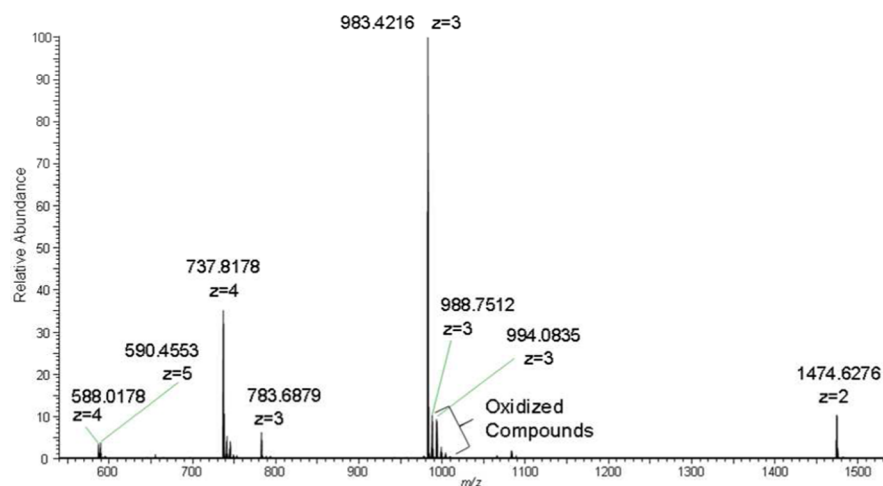
Figure 5. Electrospray ionization mass spectrum for Texas Red-labeled **HPTH59-a**.
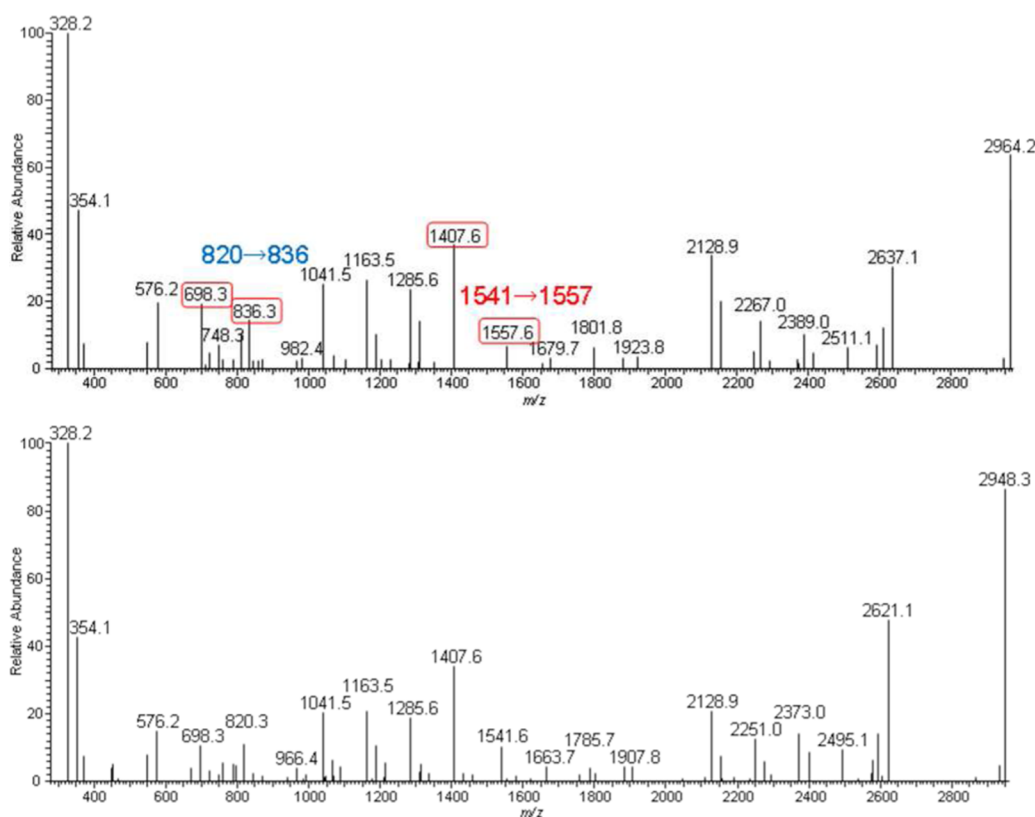

Figure 6. Upper panel shows the MS/MS spectrum of the ion at m/z 988.7524 ($[M + 3H]^{3+}$) observed as a byproduct. The 16 Da-shifted ions at m/z 836 and m/z 1,557 suggest that one oxygen atom adducted a pyrrole residue. The lower panel is an MS/MS spectrum of the synthetic target Texas Red-labeled **HPTH59-a** (m/z 983.4214: $[M + 3H]^{3+}$). Both spectra were deconvoluted to singly charged ions.

■ CONCLUSION

We conclude that the compound Dab(Im-Im-Py)-Py-Py-Py-Im-[NH(C$_2$H$_4$O)$_2$(CH$_2$)$_2$CO]-Dab(Im-Im-Py)-Py-Py-Py-Im-βAla-NH(CH$_2$)$_3$N(CH$_3$)-(CH$_2$)$_3$NH-TAMRA (TAMRA-labeled **HPTH59-b**) is the optimal probe for telomere staining. The oxidative instability of PIPAs has been identified for the first time by using high-resolution mass spectrometry. Although oxidized impurities were present in very tiny amounts, they did not influence practical applications.

■ MATERIALS AND METHODS

General. The reagents for polyamide syntheses such as Fmoc-Py-OH, Fmoc-Im-OH, Fmoc-Py-Im-OH, and Im-CCl$_3$, solid supports (Fmoc-Py-ClTrt resin, Fmoc-βAla-Wang resin), O-(1H-6-chlorobenzotriazol-1-yl)-1,1,3,3-tetramethyluronium hexafluorophosphate (HCTU), benzotriazol-1-yloxytripyrrolidinophosphonium hexafluorophosphate (PyBOP), and tetramethylrhodamine (TAMRA) succinimidyl ester were from HiPep Laboratories (Kyoto, Japan). Trifluoroacetic acid (TFA), 2,2,2-trifluoroethanol (TFE), 3,3′-diamino-N-methyldipropylamine, Texas red succinimidyl ester, N,N-diisopropylethylamine (DIEA), dichloromethane (DCM), methanol, acetic acid (AcOH), 1-methyl-2-prrrolidone (NMP), and N,N-dimethylformamide (DMF) were obtained from Nacalai Tesque (Kyoto, Japan).
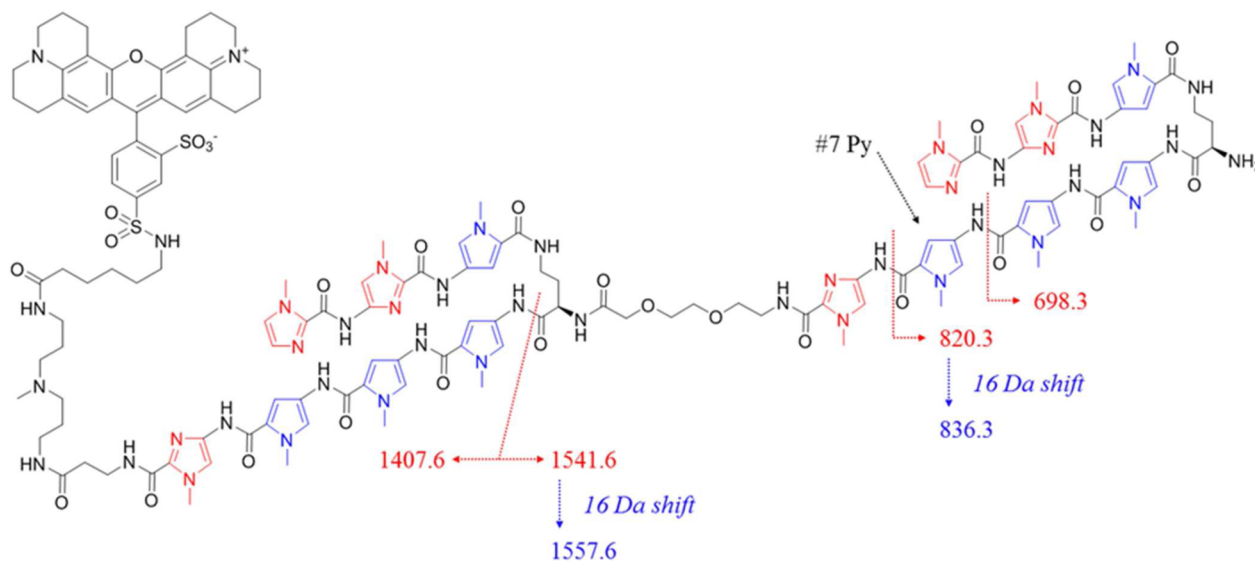
Figure 7. Identification of one of the oxidized residues in Texas Red-labeled **HPTH59-a** through high-resolution MS/MS (refer to Figure 6). One of the oxygen adducts was identified at residue no. 7 (Py).
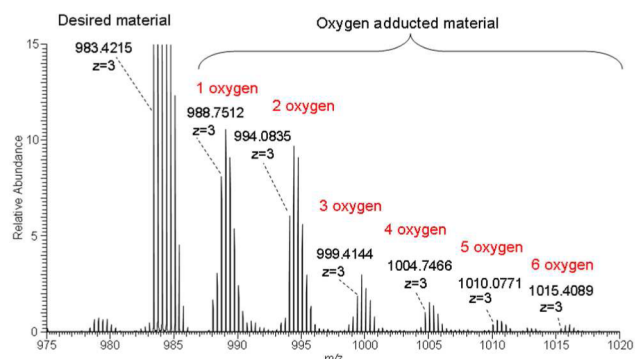

Figure 8. Identification of oxygen-adducted materials (number of oxygen atoms are indicated) on purified Texas Red-labeled **HPTH59-a.**

Fmoc-D-Dab(Boc)-OH, Fmoc-O2Oc-OH, and Fmoc-NH-dPEG(3)-COOH were obtained from Iris Biotech GmbH (Marktredwitz, Deutschland). *N*-Fmoc-amido-dPEG$_2$-acid and *N*-Fmoc-amido-dPEG$_4$-acid were obtained from Quanta Biodesign, Ltd. (San Francisco, CA). Polyamide-chain assembly was performed on an automated synthesizer, PSSM-8 (Shimadzu, Kyoto, Japan). HPLC grade acetonitrile (Nacalai tesque) was used for both analytical and preparative HPLC. Water was prepared by a Milli-Q apparatus (Millipore, Tokyo, Japan). All chemicals were used as received. Analyses by reversed-phase (RP)-HPLC were carried out online LCMS (Agilent 1100 ion-trap mass spectrometer, HCT ultra, Bruker Daltonics, Yokohama, Japan), with analytical RP-HPLC columns, HiPep-Cadenza (3.0 × 150 mm, HiPep Laboratories) or HiPep-Intrada (3.0 × 150 mm, HiPep Laboratories). Preparative purification was carried out using HiPep-Cadenza (20 × 150 mm, HiPep Laboratories) and HiPep-Intrada (20 × 250 mm, HiPep-Laboratories) with an LC-10A System (Shimadzu). UV spectra were measured on a NanoDrop 2000c (Thermo Fisher Scientific). Cell images were recorded with DeltaVision (Applied Precision). Hela 1.3 cells were generous gifts from Dr. T. de Lange (Rockefeller University). DMEM medium was purchased from Life Technology. Normal goat serum (NGS) was from Millipore. Nocodazole, paraphenylenediamine, and Triton X-100 were from Sigma. DAPI was from Roche. All other materials were from standard suppliers (highest quality available).

Synthesis of Building Block of Im-Im-Py-OH (2). Fmoc-Py-ClTrt resin (0.57 mmol/g, 5.0 g, 2.85 mmol) reacted with Fmoc-Im-OH (2.6 g, 7.13 mmol), HCTU (2.9 g, 7.13 mmol), and DIEA (2.5 mL, 14.3 mmol) in DMF for 1 h at 60 °C. After deprotection of the Fmoc group by 20% piperidine DMF solution, ImPy-ClTrt resin reacted with Im-CCl$_3$ (1.6 g, 7.13 mmol) and DIEA (2.5 mL, 14.3 mmol) in DMF for 1 h at 60 °C. After assembly, the ImImPy-ClTrt resin was washed with DMF, DCM, and MeOH and dried for overnight in vacuo. The ImImPy-ClTrt resin was cleaved by a TFE:AcOH:DCM = 1:1:3 solution. The resin was removed by filtration and washed with DCM, and the filtrate was concentrated in vacuo. The residue was triturated with water and then dried in vacuo to afford ImImPy-OH (810.9 mg, 77% yield). MS data are exhibited in Supporting Information.

Synthesis of Fmoc-D-Dab(Im-Im-Py)-OH (1). Fmoc-D-Dab-(Boc)-OH (960.3 mg, 2.18 mmol) was treated with a 90% TFA water solution (1 mL) at 1 h. After concentration of the solution, the residue was dried overnight. Meanwhile, Im-Im-Py-OH (810.9 mg, 2.18 mmol), DIEA (1.85 mL, 10.9 mmol), and PyBOP (1.13 g, 2.18 mmol) were dissolved in DMF (10 mL). The solution was added slowly to Fmoc-D-Dab(NH$_2$)-OH, and the reaction solution was stirred for 1 h at ambient temperature. The reaction solution was concentrated in vacuo. The residue was washed with diethyl ether and triturated with water. The resulting residue was purified by silica gel column chromatography (eluent DCM/methanol/DIEA = 20:1:1) and yielded the compound (592.6 mg, 39%). This compound was used in the next reaction. MS data are exhibited in Supporting Information.

Polyamide Synthesis. Polyamides were prepared by the Fmoc SPS using PSSM-8. Many of the PIPA have "difficult sequences"; therefore, we have employed improved highly efficient protocols based on those previously reported.[18] The resulting polyamidyl resin was cleaved from the solid support with 3,3′-diamino-*N*-methyldipropyl-amine for 3 h at 60 °C. Resin was filtered off, and the resulting liquor was treated with diethyl ether. The precipitated crude polyamide was washed three times with diethyl ether and analyzed by RP-HPLC. Crude polyamides were purified on a preparative column, HiPep-Intrada, at 60 °C. The purified peptides were assessed by the LCMS system described above.

Synthesis of Dab(Im-Im-Py)-Py-Py-Py-Im-Hinge-Dab(Im-Im-Py)-Py-Py-Py-Im-βAla-NH(CH$_2$)$_3$N(CH$_3$)-(CH$_2$)$_3$NH$_2$. Polyamide-chain assembly was performed on an automated synthesizer, PSSM-8. The start resin was Fmoc-β-Ala-Wang resin (18 mg, 0.57 mmol/g), and the HCTU−DIEA−NMP method (Fmoc-amino acid and HCTU: 5 equiv, DIEA: 10 equiv, coupling time: 60 min, nitrogen gas bubbling for dissolving reagents: 10 min) was used. Deprotection of Fmoc group was performed twice with 20% PIP−DMF for 5 min at ambient temperature in duplicate. The coupling took place in the order of

11552

dx.doi.org/10.1021/ja506058e | *J. Am. Chem. Soc.* 2014, 136, 11546−11554

Fmoc-Py-Im-OH, Fmoc-Py-OH, Fmoc-Py-OH, Fmoc-D-Dab(Im-Im-Py)-OH, Fmoc-Hinge-OH, Fmoc-Py-Im-OH, Fmoc-Py-OH, Fmoc-Py-OH, and Fmoc-D-Dab(Im-Im-Py)-OH. After automated assembly, the resin was washed with methanol and dried in vacuo. After that, the compound supported by Wang resin was cleaved using 3,3′-diamino-N-methyldipropylamine (0.2 mL) for 3 h at 60 °C. The resin was removed by filtration and washed with dichloromethane, and the filtrate was concentrated in vacuo. The resulting crude polyamide was purified by RP-HPLC, and appropriate fractions were collected under freeze-drying conditions to give the compound (**HPTH59-a**: 2.8 mg, 12% yield; **HPTH59-b**: 3.4 mg, 15% yield; **HPTH59-c**: 1.9 mg, 8% yield; **HPTH59-d**: 2.7 mg, 12% yield; **HPTH59-e**: 3.6 mg, 17%). MS data are exhibited in Supporting Information.

Synthesis of Dab(Im-Im-Py)-Py-Py-Py-Im-Hinge-Dab(Im-Im-Py)-Py-Py-Py-Im-βAla-NH(CH$_2$)$_3$N(CH$_3$)-(CH$_2$)$_3$NH-fluorophore. Fluorophore succinimidyl ester (1 mg/mL) in DMF was prepared. Polyamide was dissolved in DMF containing fluorophore succinimidyl ester (1 equiv) and DIEA (10 equiv). The reaction mixture was stirred for 4 h at ambient temperature with shielding from the light. The reaction mixture was purified by RP-HPLC, and appropriate fractions were collected under freeze-drying conditions to give the compound (Texas Red labeled **HPTH59-a**: 22% yield; **-b**: 12% yield; **-c**: 23% yield; **-d**: 24% yield, and **-e**: 11%, respectively; TAMRA-labeled **HPTH59-a**: 28% yield; **-b**: 19% yield; **-c**: 34% yield; **-d**: 29% yield and **-e**: 44% yield, respectively;). MS data are exhibited in Supporting Information. Fluorescent labeled polyamide concentrations were calculated with a NanoDrop 2000c using an extinction coefficient of 112000 M^{-1} cm^{-1} derived Texas Red λ_{max} near 583 nm, or 91000 M^{-1} cm^{-1} derived TAMRA λ_{max} near 545 nm.

Thermal Denaturation Analyses. Thermal denaturation analyses of the polyamide–DNA complex were performed on a V-650 spectrophotometer (JASCO) having a cell path length of 1 cm equipped with a thermocontrolled PAC-743R cell changer (JASCO) and a refrigerated and heated circulator F25-ED (Julabo) as described.[12a] The sequences of the DNAs used, purchased from Sigma-Aldrich, were 5′-GGTT<u>AGGGTTAGGGTT</u>AGG-3′ (ODN-1) and 3′-CCAAT<u>CCCAATCCCAAT</u>CC-5′ (ODN-2), 5′-GGTT<u>A-GAGTTAGGGTT</u>AGG-3′ (ODN-3) and 3′-CCAAT<u>CTCAATCC-CAA</u>TCC-5′ (ODN-4), 5′-GGTT<u>AGGGTTAGAGTT</u>AGG-3′ (ODN-5) and 3′-CCAAT<u>CCCAATCTCAA</u>TCC-5′ (ODN-6), and 5′-GGTT<u>AGAGTTAGAGTT</u>AGG-3′ (ODN-7) and 3′-CCAAT<u>CT-CAATCTCAA</u>TCC-5′ (ODN-8), which had no mismatch, a 1 bp mismatch at the side of the polyamides' C-termini, a l bp mismatch at the side of their N-termini, and a 2 bp mismatch, respectively. The underlined bases are the binding sites of the polyamides and the bold bases show mismatched parts. The analysis buffer is as follows: the aqueous solution of 10 mM sodium chloride and 10 mM sodium cacodylate at pH 7.0 containing 2.5% v/v DMF. The final concentrations of polyamides and dsDNA were 12.5 μM and 2.5 μM, respectively (5:1 stoichiometry). Before analyses, mixed samples (total: 120 μL) were heated to 95 °C and then annealed to 25 °C at a rate of 1.0 °C/min. Denaturation profiles were recorded at λ = 260 nm from 25 to 95 °C at a rate of 1.0 °C/min, and melting temperatures were measured as the maximum of the first derivative of the profiles. Reported values were the averages of at least three measurements.

SPR Assays. The SPR assays were performed using a BIACORE X instrument as previously described.[7e,17] Biotinylated hairpin DNA purchased from JBioS, whose sequence was 5′-biotin-GGTTAGGGT-TAGGGTTAGGTTTTCCTAACCCTAACCCTAACC-3′, was im-mobilized on streptavidin-coated sensor chip SA to obtain the desired immobilization level (approximately 900 RU rise). The assays were carried out using HBS-EP (10 mM HEPES (pH 7.4), 150 mM NaCl, 3 mM EDTA, 0.005% v/v Surfactant P20), purchased from GE Healthcare, with 0.1% DMSO at 25 °C. A series of sample solutions with various concentrations were prepared in the buffer with 0.1% DMSO and injected at a flow rate of 20 mL/min. To calculate the association rate (k_a), dissociation rate (k_d), and dissociation constant (K_D), data processing was performed with 1:1 binding with mass a transfer model using BIAevaluation 4.1 program. The closeness of fit is described by the statistical value χ^2:

$$\chi^2 = \frac{\sum_1^n (r_f - r_x)^2}{n - p}$$

where r_f is the fitted value at a given point, r_x is the experimental value at the same point, n is the number of data points, and p is the number of fitted parameters.[7e]

Telomere Staining of HeLa 1.3 Cell Spreads with Fluorescent Polyamides. HeLa 1.3 cells were maintained at 37 °C (5% CO$_2$) in DMEM containing 10% FBS. HeLa 1.3 cells were blocked mitotically by adding 0.1 μg/mL nocodazole for 4 h. The cells were swollen by treatment with a hypotonic buffer (0.075 M KCl) for 15 min at room temperature and fixed with a methanol/acetic acid (3:1) solution for 5 min. After centrifugation, the cell pellet was again suspended in the methanol/acetic acid solution. The cell suspension was spread on coverslips and air-dried at room temperature for 5 min and at 60 °C for 30 min. The cell spread coverslips were kept at 4 °C until use. The air-dried spread coverslips were soaked in TEN buffer (10 mM Tris-HCl pH 7.5, 1 mM EDTA, 100 mM NaCl) overnight at 4 °C before use. For blocking, the spread coverslips were treated with 10% NGS in TE buffer for 30 min at room temperature. After brief washing with TE buffer, the spread coverslips were incubated with 10% NGS, 10 nM polyamide in DMF, and 0.5 μg/mL DAPI in TE buffer at room temperature for 1 h and followed by five washes (3 min) with TEN buffer. The cell spreads coverslips were mounted in PPDI solution (10 mM HEPES pH 7.5, 100 mM KCl, 1 mM MgCl$_2$, 80% glycerol, 1 mg/mL paraphenylenediamine),[19] and the coverslips were sealed with a nail polish. Sectioning images were recorded with DeltaVision and projected ("Quick Projection" tool) without deconvolution to obtain telomeric signals and background signals.[19]

Telomere Staining of Formaldehyde-Fixed HeLa 1.3 Cells with Fluorescent Polyamides. For polyamide staining, the HeLa cells were grown on coverslips coated with polylysine. The cell coverslips were washed in phosphate-buffered saline (PBS) twice and fixed with 1.85% formaldehyde in PBS for 15 min at room temperature. The fixed cell coverslips were then treated with 50 mM glycine in PBS for 5 min and permeabilized with 0.5% Triton X-100 in PBS for 5 min. After briefly washing with HMK buffer (10 mM HEPES pH 7.5, 1 mM MgCl$_2$, 100 mM KCl) twice, the coverslips were incubated in HEN buffer (10 mM HEPES pH 7.5, 1 mM EDTA, 100 mM NaCl) at 37 °C overnight and kept at 4 °C until use. For blocking, the cell coverslips were treated with 10% NGS in TE buffer (10 mM Tris-HCl pH 7.5, 1 mM EDTA) for 30 min at room temperature. After a brief rinse with TE buffer, the cells were incubated with 10% NGS, 10 nM polyamide in DMF, and 0.5 μg/mL DAPI in TE buffer at 37 °C for 1 h. After washing with TEN200 buffer (10 mM Tris-HCl pH7.5, 1 mM EDTA, and 200 mM NaCl) (five times for 3 min), the mounting and subsequent image acquisitions were performed as described above. For quantification of the telomere signals in Figure 4, they were extracted from Figure 3B images as described previously.[10] The telomere signals yielded by the polyamides were extracted based on threshold values using the Softworks software (Applied Precision). The maximum intensity values of signals in the extracted telomere regions were then used as telomere signals. For the background signals, 10 squares (10 pixels × 10 pixels) were randomly set outside the defined telomere signals, and mean values of the signals in the squares were used as background signals.

Microheterogeneity Analyses. Mass spectrometry: PIPA was analyzed using mass spectrometer (LTQ Orbitrap velos, Thermo Scientific) coupled with nano-LC (EASY-nLC II, Theromo Scientific). The nano LC column was NANO HPLC CAPILLARY COLUMN (0.075 mm i.d. × 100 mm, Nikkyo Technos). Eluent A was 0.1% trifluoroacetic acid (TFA) containing distilled water. Eluent B was 0.1% TFA containing 70% acetonitrile. The gradient of eluent was programmed as linear gradient through 20 min from 0% to 100% of B eluent. Mass spectrum was obtained using Orbitrap analyzer. High resolution MS/MS spectrum was obtained using Orbitrap analyzer by collision-induced dissociation at the quadrupole collision cell with 35 V collision voltage.

■ ASSOCIATED CONTENT

ⓢ Supporting Information

Mass spectra of the polyamide compounds and derivatives, thermal denaturation profiles of **HPTH59a−e**, comparative SPR analysis, mass chromatogram of Texas Red-labeled **HPTH59-a**. This material is available free of charge via the Internet at http://pubs.acs.org.

■ AUTHOR INFORMATION

Corresponding Author

noki@hipep.jp

Notes

The authors declare no competing financial interest.

■ ACKNOWLEDGMENTS

■ REFERENCES

(1) (a) White, S.; Szewczyk, J. W.; Turner, J. M.; Baird, E. E.; Dervan, P. B. *Nature* **1998**, *391*, 468−471. (b) Trauger, J. W.; Baird, E. E.; Dervan, P. B. *Nature* **1996**, *382*, 559−561. (c) Dervan, P. B.; Bürli, R. W. *Curr. Opin. Chem. Biol.* **1999**, *3*, 688−693. (d) Dervan, P. B. *Bioorg. Med. Chem.* **2001**, *9*, 2215−2235. (e) Dervan, P. B.; Edelson, B. S. *Curr. Opin. Struct. Biol.* **2003**, *13*, 284−299. (f) Dervan, P. B.; Doss, R. M.; Marques, M. A. *Curr. Med. Chem.: Anti-Cancer Agents* **2005**, *5*, 373−387. (g) Blackledge, M. S.; Melander, C. *Bioorg. Med. Chem.* **2013**, *21*, 6101−6114.

(2) Turner, J. M.; Swalley, S. E.; Baird, E. E.; Dervan, P. B. *J. Am. Chem. Soc.* **1998**, *120*, 6219−6226.

(3) (a) Swalley, S. E.; Baird, E. E.; Dervan, P. B. *J. Am. Chem. Soc.* **1999**, *121*, 1113−1120. (b) Herman, D. M.; Baird, E. E.; Dervan, P. B. *J. Am. Chem. Soc.* **1998**, *120*, 1382−1391.

(4) (a) Baird, E. E.; Dervan, P. B. *J. Am. Chem. Soc.* **1996**, *118*, 6141−6146. (b) Wurtz, N. R.; Turner, J. M.; Baird, E. E.; Dervan, P. B. *Org. Lett.* **2001**, *3*, 1201−1203. (c) Puckett, J. W.; Green, J. T.; Dervan, P. B. *Org. Lett.* **2012**, *14*, 2774−2777. (d) Chenoweth, D. M.; Harki, D. A.; Dervan, P. B. *J. Am. Chem. Soc.* **2009**, *131*, 7175−7181.

(5) (a) Bando, T.; Sugiyama, H. *Acc. Chem. Res.* **2006**, *39*, 935−944. (b) Xiao, X.; Yu, P.; Lim, H. S.; Sikder, D.; Kodadek, T. *Angew. Chem., Int. Ed.* **2007**, *46*, 2865−2868. (c) Chenoweth, D. M.; Dervan, P. B. *J. Am. Chem. Soc.* **2010**, *132*, 14521−14529. (d) Meier, J. L.; Yu, A. S.; Korf, I.; Segal, D. J.; Dervan, P. B. *J. Am. Chem. Soc.* **2012**, *134*, 17814−17822. (e) Vaijayanthi, T.; Bando, T.; Pandian, G. N.; Sugiyama, H. *ChemBioChem.* **2012**, *13*, 2170−2185. (f) Singh, I.; Wendeln, C.; Clark, A. W.; Cooper, J. M.; Ravoo, B. J.; Burley, G. A. *J. Am. Chem. Soc.* **2013**, *135*, 3449−3457. (g) Pandian, G. N.; Taniguchi, J.; Junetha, S.; Sato, S.; Han, L.; Saha, A.; Anandhkumar, C.; Bando, T.; Nagase, H.; Vaijayanthi, T.; Taylor, R. D.; Sugiyama, H. *Sci. Rep.* **2014**, *4*, 3843.

(6) (a) Mrksich, M.; Parks, M. E.; Dervan, P. B. *J. Am. Chem. Soc.* **1994**, *116*, 7983−7988. (b) de Clairac, R. P. L.; Geierstanger, B. H.; Mrksich, M.; Dervan, P. B.; Wemmer, D. E. *J. Am. Chem. Soc.* **1997**, *119*, 7909−7916.

(7) (a) Trauger, J. W.; Baird, E. E.; Mrksich, M.; Dervan, P. B. *J. Am. Chem. Soc.* **1996**, *118*, 6160−6166. (b) Trauger, J. W.; Baird, E. E.; Dervan, P. B. *J. Am. Chem. Soc.* **1998**, *120*, 3534−3535. (c) Weyermann, P.; Dervan, P. B. *J. Am. Chem. Soc.* **2002**, *124*, 6872−6876. (d) Poulin-Kerstien, A. T.; Dervan, P. B. *J. Am. Chem. Soc.* **2003**, *125*, 15811−15821. (e) Yamamoto, M.; Bando, T.; Morinaga, H.; Kawamoto, Y.; Hashiya, K.; Sugiyama, H. *Chem.—Eur. J.* **2014**, *20*, 752−759.

(8) (a) Herman, D. M.; Baird, E. E.; Dervan, P. B. *Chem.—Eur. J.* **1999**, *5*, 975−983. (b) Kers, I.; Dervan, P. B. *Bioorg. Med. Chem.* **2002**, *10*, 3339−3349. (c) Schaal, T. D.; Mallet, W. G.; McMinn, D. L.; Nguyen, N. V.; Sopko, M. M.; John, S.; Parekh, B. S. *Nucleic Acids Res.* **2003**, *31*, 1282−1291. (d) Sasaki, S.; Bando, T.; Minoshima, M.; Shinohara, K.; Sugiyama, H. *Chem.—Eur. J.* **2008**, *18*, 864−870.

(9) (a) Blackburn, E. H. *Angew. Chem., Int. Ed.* **2010**, *49*, 7405−7421. (b) Nandakumar, J.; Cech, T. R. *Nat. Rev. Mol. Cell Biol.* **2013**, *14*, 69−82. (c) Zakian, V. A. *Exp. Cell Res.* **2012**, *318*, 1456−1460. (d) Smogorzewska, A.; de Lange, T. *Annu. Rev. Biochem.* **2004**, *73*, 177−208.

(10) Maeshima, K.; Janssen, S.; Laemmli, U. K. *EMBO J.* **2001**, *20*, 3218−3228.

(11) Lansdorp, P. M.; Verwoerd, N. P.; van de Rijke, F. M.; Dragowska, V.; Little, M. T.; Dirks, R. W.; Raap, A. K.; Tanke, H. J. *Hum. Mol. Genet.* **1996**, *5*, 685−691.

(12) (a) Kawamoto, Y.; Bando, T.; Kamada, F.; Li, Y.; Hashiya, K.; Maeshima, K.; Sugiyama, H. *J. Am. Chem. Soc.* **2013**, *135*, 16468−16477. (b) Yamamoto, M.; Bando, T.; Kawamoto, Y.; Taylor, R.; Hashiya, K.; Sugiyama, H. *Bioconjugate Chem.* **2014**, *25*, 552−559.

(13) Fujimoto, K.; Iida, H.; Kawakami, M.; Bando, T.; Tao, Z. F.; Sugiyama, H. *Nucleic Acids Res.* **2002**, *30*, 3748−3753.

(14) Lai, Y.-M.; Fukuda, N.; Ueno, T.; Kishioka, H.; Matsuda, H.; Saito, S.; Matsumoto, K.; Ayame, H.; Bando, T.; Sugiyama, H.; Mugishima, H.; Serie, K. *J. Pharmacol. Exp. Ther.* **2005**, *315*, 571−575.

(15) Yasuhara, T.; Nokihara, K. *Anal. Chem.* **1998**, *70*, 3505−3509.

(16) (a) Pilch, D. S.; Poklar, N.; Gelfand, C. A.; Law, S. M.; Breslauer, K. J.; Baird, E. E.; Dervan, P. B. *Proc. Natl. Acad. Sci. U. S. A.* **1996**, *93*, 8306−8311. (b) Muzikar, K. A.; Meier, J. L.; Gubler, D. A.; Raskatov, J. A.; Dervan, P. B. *Org. Lett.* **2011**, *13*, 5612−5615.

(17) (a) Zhang, W.; Bando, T.; Sugiyama, H. *J. Am. Chem. Soc.* **2006**, *128*, 8766−8776. (b) Morinaga, H.; Bando, T.; Takagaki, T.; Yamamoto, M.; Hashiya, K.; Sugiyama, H. *J. Am. Chem. Soc.* **2011**, *133*, 18924−18930.

(18) (a) Nokihara, K.; Nagawa, Y.; Hong, S.-P.; Nakanishi, H. *Lett. Pept. Sci.* **1997**, *4*, 141−146. (b) Nokihara, K.; Yasuhara, T.; Nakata, Y.; Lerner, E. A.; Wray, V. *Int. J. Pept. Res. Ther.* **2007**, *13*, 377−386.

(19) (a) Maeshima, K.; Laemmli, U. K. *Dev. Cell* **2003**, *4*, 467−480. (b) Maeshima, K.; Yahata, K.; Sasaki, Y.; Nakatomi, R.; Tachibana, T.; Hashikawa, T.; Imamoto, F.; Imamoto, N. *J. Cell Sci.* **2006**, *119*, 4442−4451.